NMR solution structure of the reduced form of thioredoxin 2 from Saccharomyces cerevisiae

ARTICLE *in* JOURNAL OF BIOMOLECULAR NMR · JUNE 2007

Impact Factor: 3.14 · DOI: 10.1007/s10858-007-9144-z · Source: PubMed

J Biomol NMR (2007) 38:99–104
DOI 10.1007/s10858-007-9144-z

NMR STRUCTURE NOTE

NMR solution structure of the reduced form of thioredoxin 2 from *Saccharomyces cerevisiae*

Gisele Cardoso Amorim · Anderson Sá Pinheiro · Luis Eduardo Soares Netto · Ana Paula Valente · Fabio C. L. Almeida

Received: 19 October 2006 / Accepted: 8 January 2007 / Published online: 6 March 2007

Keywords NMR · *Saccharomyces cerevisiae* · Structure · Thioredoxin 2 · Yeast

Abbreviations
Trx thioredoxin

Biological context

Thioredoxins (Trxs) are ubiquitous heat-stable proteins of molecular mass approximately 12,000 Da that function as dithiol oxidoreductases, and are important for cellular defense against oxidative stress (Monje-Casas et al. 2004). Trxs act as hydrogen donors for reductive enzymes such as ribonucleotide reductases (Laurent et al. 1964) and thioredoxin peroxidases (Kang et al. 1998), as a general reductant for disulfides in proteins (Holmgren 1985), and as regulatory factors for enzymes or receptors in photosynthetic systems (Buchanan 1991). They also promote DNA binding of transcription factors, such as NF-κB and YAP-1 (Schenk et al. 1994), among others.

In yeast, there are two cytoplasmic (Trx1 and Trx2) and one mitochondrial (Trx3) isoforms. Some authors consider that the preservation of the two cytoplasmic isoforms during evolution is not related to function, meaning that they are redundant. Recently, Monje-Casas et al. (2004) described some differences in expression levels under normal and oxidative stress conditions. The basal level of both thioredoxins is the same, but becomes different after treatment with hydrogen peroxide. Trx2 shows an increase of 14 fold in its expression, whereas Trx1 remains unaffected.

Gene duplication is widespread, but it is not always preserved in evolution. In *Saccharomyces cerevisiae* there might be an explanation for the preservation of both Trx1 and Trx2. The parallel evolution of yeast thioredoxins occurred possibly because they exerted different regulatory function. Since regulation occurs through binding to different cellular targets, Trx1 and Trx2 might be specialized to bind to different targets.

Three-dimensional structures of several thioredoxins have been determined. We have determined the NMR structure of the two cytoplasmic isoforms. In this note, we report the structure of thioredoxin 2 (PDB ID: 2HSY) and compare it to other thioredoxins.

Methods and results

Expression and purification

Individual colonies of the transformants were grown in LB medium containing 100 μg/ml ampicillin at 37°C for

G. C. Amorim · A. S. Pinheiro · A. P. Valente · F. C. L. Almeida
Centro Nacional de Ressonância Magnética Nuclear-Instituto de Bioquímica Médica-CCS, Universidade Federal do Rio de Janeiro, Rio de Janeiro, RJ, Brazil

L. E. S. Netto
Instituto de Biociências, Universidade de São Paulo, Sao Paulo, SP, Brazil

F. C. L. Almeida (✉)
Avenida Brigadeiro Trompowski, Cidade Universitária, s/n – CCS – Bloco E – Sala 10 – Ilha do Fundão, Rio de Janeiro, RJ 21941-590, Brazil
e-mail: falmeida@cnrmn.bioqmed.ufrj.br

5 h. A 1 ml aliquot of the culture was diluted on 50 ml minimal M9-medium (without labeling) and incubated overnight. This was then sub-cultured in 1 L of minimal M9-medium supplemented with thiamine, $^{15}NH_4Cl$ and/or ^{13}C-glucose as the sole nitrogen and carbon sources, to an OD of 0.8 at 600 nm and induced with 1 mM isopropyl β-D-1-thiogalactopyranoside (IPTG). The induced cells were resuspended in 50 ml of 20 mM phosphate buffer pH 8.0 containing lysozyme (1 mg/ml), methylsulphonylfluoride (PMSF) and 3 mM 2-mercaptoethanol. After 30 min of incubation on ice, the lysate was sonicated ten times for 30 s on ice. The soluble fraction was analyzed on 18% SDS-PAGE. The lysate was then heated at 90°C for 10 min. The soluble fraction was loaded to an ion-exchange column chromatography DEAE-Toyopearl 650M. Sample purity was verified by SDS-PAGE. The NMR sample was prepared in 20 mM phosphate buffer pH 7.0, 10% D_2O and 10 mM deuterated dithiothreitol (DTT).

NMR measurements

The sequential assignments of the backbone resonances were obtained from 3D triple resonance spectra HNCA, HN(CO)CA, HNCACB, HN(CO)-CACB, HNCO (Bax and Grzesiek 1993) and 2D ^{15}N-HSQC. Residual gaps and ambiguities were resolved using ^{15}N-TOCSY-HSQC and ^{15}N-NOESY-HSQC. The chemical shifts of carbons and hydrogens from non-aromatic side chains were assigned with 3D HCCH-TOCSY (Fesik et al. 1990), HCCCONH, CCCONH (Montelione and Wagner 1990) and ^{13}C-HSQC spectra. Assignments of aromatic side chains were obtained using NOEs between the aromatic protons and the βCH_2 group in the ^{13}C-NOESY-HSQC spectrum. The complete resonances of aromatic spin systems were assigned with ^{13}C-HSQC and 2D ^1H-^1H-TOCSY and NOESY spectra, done with a 100% D_2O sample. The complete assignment has been deposited in the BioMagResBank (accession number 6913, Pinheiro et al. 2006).

^{15}N-^1H heteronuclear NOE experiments were performed in a ^1H resonance frequency of 600.04 MHz using echo-antiecho for frequency discrimination in the indirect dimension, with sensitivity improvement, 1,024 complex points in the ^1H dimension and 256 in the ^{15}N dimension. The spectra were acquired with and without saturation (4s) in an interleaved fashion.

All spectra have been acquired on a Bruker DRX 600 MHz spectrometer at 30°C, processed using NMRPipe (Delaglio et al. 1995) and analyzed in NMRView 5.0.3 (Johnson and Blevins 1994).

Structure determination

Structure calculation was done using the program CNS-solve 1.1 (Brunger et al. 1998). A total of 2177 NOEs, 26 hydrogen bonds and 59 dihedral angles restraints were used to calculate a family of structures (Table 1). The solution structure of Trx2 displayed five parallel and anti-parallel β-sheets surrounded by four α-helices and an exposed active-site loop (Fig. 1), very similar to the structure of thioredoxins previously described (Katti et al. 1990; Jeng et al. 1994).

The Ramachandran plot was analyzed using PROCHECK-NMR (Laskowski et al. 1996). Table 1 shows the structural statistics. Root mean square deviation (RMSD) values from the average structure were calculated using the program MOLMOL (Koradi et al. 1996). Superposition of the backbone of residues 1 to 104 resulted in a RMSD of 0.66 Å for the 20 lowest energy structures. For the active site (W30 to C34) and the loop between residues 57 e 62, which participate in the interaction with cellular targets, the RMSD values were 0.41 and 0.52 Å, respectively.

The structures of Trx2 were compared with other thioredoxins using the software DALI (Holm and Sander 1995). Three-dimensional similarity is defined by the Z-score, which varied from 4 to 16. High

Table 1 Table of statistic for the ensemble of 20 calculated structures

Parameter	Value
Number of restraints	
NOE	
Total	2181
Intraresidue	1050
Sequential	438
medium range	252
long range	441
hydrogen bonds	26
dihedral angles	59
NOE violations >0.2 (Å)	0
rmsd (Å)	0.0071 ± 0.0003
Dihedral violations >1.0 (°)	0
rmsd (degree)	0.1963 ± 0.0353
Energy (Kcal/mol)	–171.59 ± 7.09
RMSD	
Backbone (C′, Cα e N) (Å)	
all residues	0.66
active site loop (30–34)	0.41
Heavy atoms	
all residues	1.02
active site loop (30–34)	0.8
Ramachandram (%)	
most favoured regions	68.1
additionally allowed regions	27.6
generously allowed regions	3.1
disallowed regions	1.2

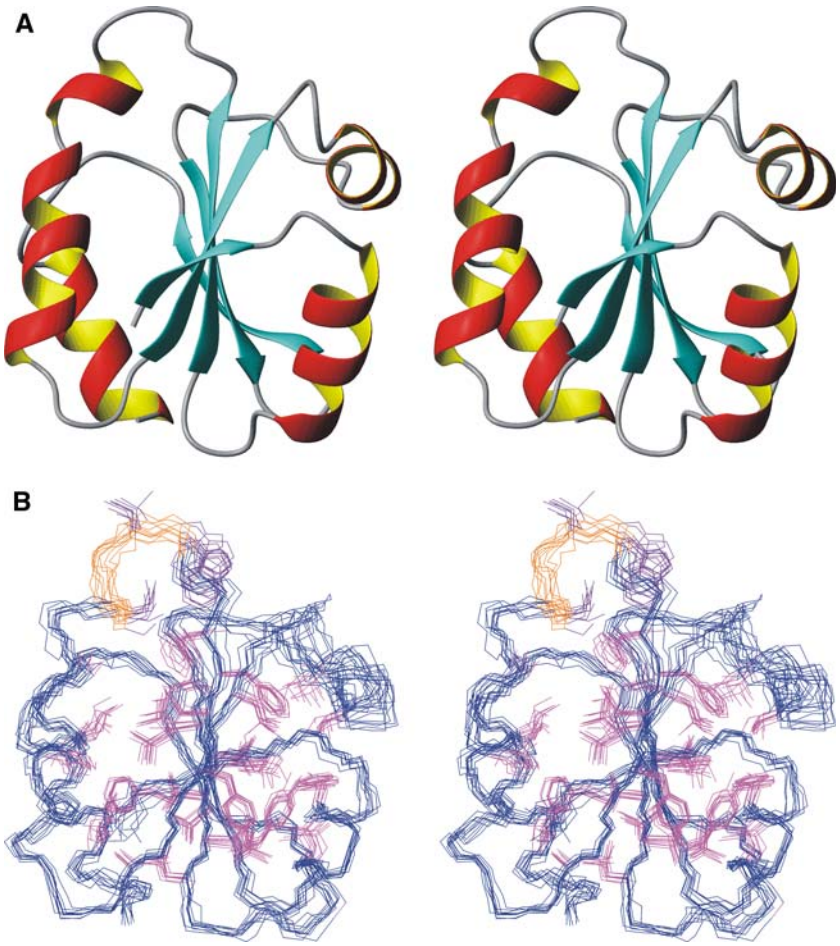

Fig. 1 (**A**) Ribbon representation of the lowest energy structure of Trx2 (stereoview). (**B**) Stereoview of the superposition of the 10 lowest energy structures of thioredoxin 2. The backbone is colored in blue. The side chains of the residues forming the hydrophobic core are shown in magenta. The side chain of the residues W30, C31 and C34, in the active site, are colored in green

Z-scores were obtained for thioredoxins of eukariotes and prokaryotes, with the exception of bacteriophages and archea. Z-scores were high for protozoa (*P. falciparum*: 15.8; *T. brucei*: 14), algae (*C. reinhardtii* H: 15.8), insects (*D. melanogaster*: 15), mammals (*H. sapiens*: 14.9), plants (*S. oleracea*: 13.9; *Anabaena sp*: 13.5) and bacteria (*T. thermophilus*: 14; *B. acidocaldarius*: 13.8, *S. coelicolor*: 13.3; *E. coli*: 13.1). Low Z-score were obtained for archea and virus (*M. thermoautotropicum*: 4.3; T4 bacteriophage: 4.7).

In addition to the comparison by DALI, based on the overall folding, we compared thioredoxins based on the RMSD per residue in an attempt to better correlate structure-function relationship among Trxs (Fig. 2).

Trx2 structure showed important structural differences between residues 28 and 35 (active-site loop) and the loop containing residues 57 to 62, known to participate in the interaction of thioredoxins with cellular targets, such as NF-κB and *E. coli* DNA polymerase (Qin et al. 1995; Doublie et al. 1998). Understanding the structural diversity of the interacting loops is important to differentiate thioredoxin function in different species.

The high RMSD observed in Fig. 2 for the interacting loops can be a result of either backbone flexibility or structural differences. To map the backbone flexibility we carried out a ^{15}N-^{1}H heteronuclear NOE (Fig. 3). All the residues involved in the secondary structure displayed ^{15}N-^{1}H NOE of approximately 0.8, typical of the well-structured residues. Eight residues displayed lower values ^{15}N-^{1}H NOE, indicating flexibility in the timescale of pico to nanoseconds, characteristic of thermal motions. All of them were located in loops of the protein. The active site loop (28-ATWCGPCK-35) showed one point of backbone flexibility in the K35. The second interacting loop (57-DVDEVS-62) showed one point of flexibility in the S62. The third interacting loop (68-AEVSSMP-74) showed S71 as the point of flexibility. The most flexible loop was the one between the residues 17 and 20.

All interacting loops contained residues undergoing thermal motions that could originate the differences in RMSD observed in Fig. 2. However, we also observed

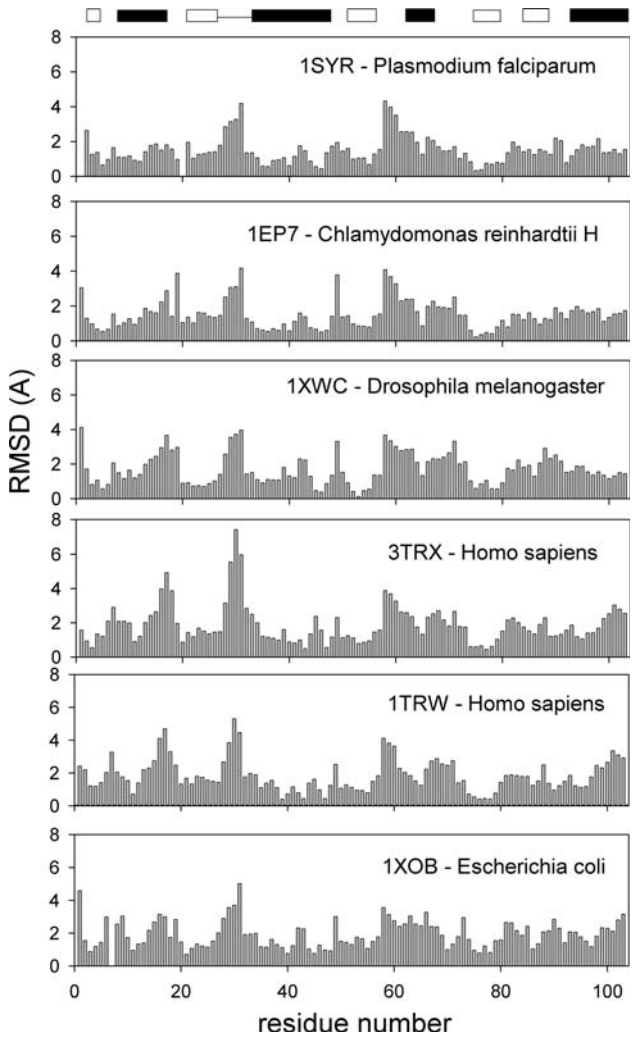

Fig. 2 Backbone RMSDs per residue calculated from the superposition of the backbone of Trx2 with other five thioredoxins in the reduced form. The alignment was the same used by the software DALI. The selection of the protein was based on the highest Z-scores, with the exception of *E. coli* thioredoxin that was included because it was extensively studied. Note that high RMSD was observed for the regions of active site and the loop between strand 3 and helix 3. Secondary structure regions displayed low RMSD. The β-strands are represented as open bars and the helices as black bars. 1SYR (Robien et al. 2004 unpublished), 1EP7 (Menchise et al. 2001), 1XWC (Wahl et al. 2005), 3TRX (Forman-Kay et al. 1991), 1TRW (Qin et al. 1994), 1XOB (Jeng et al. 1994)

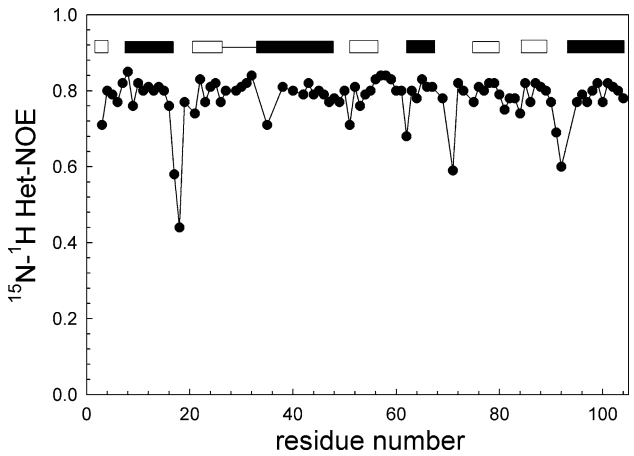

Fig. 3 ^{15}N-^{1}H heteronuclear NOE intensity ratio as a function of the residue number. The NOE intensity ratio is the relation between the spectrum acquired with ^{1}H saturation and without saturation. C34 is missing because of the extensive line broadening. The β-strands are represented as open bars and the helices as black bars

line broadening for several residues within the active-site loop, including C31 and G32. C34 was so broadened that it could not be observed in the HSQC spectrum. W30 side chain indolic resonance was duplicated, due to slow-intermediate exchange. This behavior is a result of conformational exchange in the timescale of milli to microseconds and indicates the presence of conformational diversity for this loop. We also observed several NOEs for the triad T29, W30 and C31 what suggest some degree of order within this loop. The second interacting loop also displayed complex motional behavior. We observed line broadening for the residues V61 and S62, indicating conformational diversity. Considerable line broadened resonances was also observed for S71, S72 and M73 within the third interacting loop.

Discussion and conclusions

The structures of several thioredoxins have been determined by NMR or X-ray crystallography (Katti et al. 1990; Jeng et al. 1994; Qin et al. 1994). Recently Bao et al. (2007) reported the crystal structure at 2.38 Å resolution of the oxidized yeast Trx2 (2FA4). Crystalline Trx2 is dimeric and the authors suggested the dimerization might be a mechanism to protect that active-site cysteines in the absence of a cellular target. We reported here the first solution structure for the reduced form of yeast Trx2, which was monomeric in the millimolar concentration.

We solved the structure of the reduced form of yeast thioredoxin 2, searching for a better understanding of the catalytic mechanisms and specificity differences between thioredoxins and cytoplasmic yeast thioredoxins. Surface loops commonly contain the structural determinants of substrate specificity, and this facilitates rapid evolutionary divergence and adaptation since the loops can vary, whereas the structural integrity of the protein fold is maintained (Perona and Craik 1997). Comparing the primary sequence of Trx2

with other thioredoxins, we found 78% of identity with Trx1, and high homology to thioredoxins from fungi and mammals (30–48%). As expected, comparison of the tertiary structures showed that Trx2 is very similar to all other thioredoxins, with the exception of thioredoxins from phages and archea. We suggest that the comparison of the structures should be done not by overall folding but by looking at individual regions of the protein, such as the interacting loops. Analysis of heteronuclear NOE and the line broadening of each individual resonances indicated the interacting loops undergo a complex mode of motions that involves one point of flexibility in the backbone, occurring in the timescale of pico to nanoseconds, and the switch between ordered conformational states, occurring in the timescale of milli to microseconds.

The conformational differences observed between different species depicted in Fig. 2 may be a result of not only flexibility but of a more complex motion involving a conformational switch between ordered conformational states. The presence of conformational diversity of a protein in its free state frequently occurs in regions involved in binding or allostery (Valente et al. 2006). New efforts must be done to understand structural diversity in the interacting loops of thioredoxins.

Acknowledgements This work was supported by Conselho Nacional de Desenvolvimento Científico e Tecnológico (CNPq), Programas de Núcleos de Excelência (CNPq/PRONEX), Fundação Carlos Chagas Filho de Amparo à Pesquisa do Estado do Rio de Janeiro (FAPERJ) and Coordenação de Aperfeiçoamento de Pessoal de Nível Superior (CAPES). We thank Dr. Catarina Akiko Miyamoto and Prof. Franklin Rumjanek for the english review.

References

Bao R, Chen Y, Tang YJ, Janin J, Zhou CZ (2007) Crystal structure of the yeast cytoplasmic thioredoxin Trx2. Proteins 66:246–249

Bax A, Grzesiek S (1993) Methodological advances in protein NMR. Acc Chem Res 26:131–138

Brunger AT, Adams PD, Clore GM, Delano WL, Gros P, Grosse-Kunstleve RW, Jiang JS, Kuszewski J, Nilges N, Pannu NS, Read RJ, Rice LM, Simonson T, Warren GL (1998) Crystallography & NMR system: A new software suite for macromolecular structure determination. Acta Cryst D 54:905–921

Buchanan BB (1991) Regulation of CO_2 assimilation in oxygenic photosynthesis—the ferredoxin thioredoxin system—Perspective on its discovery, present status, and future-development. Arch Biochem Biophys 288:1

Delaglio F, Grzesiek S, Vuister GW, Zhu G, Pfeifer J, Bax A (1995) NMR Pipe—a multidimensional spectral processing system based on unix pipes. J Biomol NMR 6:277–293

Doublie S, Tabor S, Long AM, Richardson CC, Ellenberger T (1998) Crystal structure of a bacteriophage T7 DNA replication complex at 2.2 angstrom resolution. Nature 391:251–258

Fesik SW, Eaton HL, Olejniczak ET, Zuiderweg ERP, McIntosh LP, Dahlquist FW (1990) 2D and 3D NMR-spectroscopy employing C-13-C-13 magnetization transfer by isotropic mixing—Spin system-identification in large proteins. J Am Chem Soc 112:886–888

Forman-Kay JD, Clore GM, Wingfield PT, Gronenborn AM (1991) High-resolution 3-dimensional structure of reduced recombinant human thioredoxin in solution. Biochemistry (USA) 30:2685–2698

Holm L, Sander C (1995) DALI - A network tool for protein-structure comparison. Trends Biochem Sci 20(11):478–480

Holmgren A (1985) Thioredoxin. Annu Rev Biochem 54:237–271

Jeng MF, Campbell AP, Begley T, Holmgren A, Case DA, Wright PE, Dyson HJ (1994) High-resolution solution structures of oxidized and reduced *Escherichia coli* thioredoxin. Structure 2(9):853–868

Johnson BA, Blevins RA (1994) NMR View—a computer-program for the visualization and analysis of NMR data. J Biomol NMR 4:603–614

Kang SW, Chae HZ, Seo MS, Rhee SG (1998) Mammalian peroxiredoxin isoforms can reduce hydrogen peroxide generated in response to growth factors and tumor necrosis factor-alpha. J Biol Chem 273:6297–6302

Katti SK, Lemaster DM, Eklund H (1990) J Mol Biol 212(1):167–184

Koradi R, Billeter M, Wuthrich K (1996) Crystal-structure of thioredoxin from *Escherichia coli* at 1.68A resolution. J Mol Graph 14:51–55, 29–32

Laskowski RA, Rullmann JAC, MacArthur MW, Kaptein R, Thornton JM (1996) AQUA and PROCHECK-NMR: Programs for checking the quality of protein structures solved by NMR. J Biomol NMR 8(4):477–486

Laurent TC, Moore EC, Reichard P (1964) Enzymatic synthesis of deoxyribonucleotides. Isolation + characterization of thioredoxin hydrogen donor from *Escherichia coli* B. J Biol Chem 239:3436–3444

Menchise V, Corbier C, Didierjean C, Saviano M, Benedetti E, Jacquot JP, Aubry A (2001) Crystal structure of the wild-type and D30A mutant thioredoxin of *Chlamydomonas reinhardtii* and implications for the catalytic mechanism. Biochem J 359:65–75

Monje-Casas F, Michan C, Pueyo C (2004) Absolute transcript levels of thioredoxin- and glutathione-dependent redox systems in *Saccharomyces cerevisiae*: response to stress and modulation with growth. Biochem J 383:139–147

Montelione GT, Wagner G (1990) Conformation-independent sequential NMR connections in isotope-enriched polypeptides by H-1-C-13-N-15 triple-resonance experiments. J Magn Reson 87:183–188

Perona JJ, Craik CS (1997) Evolutionary divergence of substrate specificity within the chymotrypsin-like serine protease fold. J Biol Chem 272(48):29987–29990

Pinheiro AS, Amorim GC, Netto LE, Valente AP, Almeida FCL (2006) (1) H, (13) C and (15) N Resonance assignments for the reduced forms of thioredoxin 1 and 2 from *S. cerevisiae*. J Biomol NMR 36(5):35

Qin J, Clore GM, Gronenborn AM (1994) The high-resolution 3-dimensional solution structures of the oxidized and reduced states of human thioredoxin. Structure 2:503–522

Qin J, Clore GM, Kennedy WM, Huth JR, Gronenborn AM (1995) Solution structure of human thioredoxin in a mixed disulfide intermediate complex with its target peptide from the transcription factor NF-kappa-B. Structure 3:289–297

Schenk H, Klein M, Erdbrugger W, Droge W, Schulze-Osthoff K (1994) Distinct effects of thioredoxin and antioxidants on the activation of transcription factors NF-kappa-B and AP-1. Proc Natl Acad Sci USA 91:1672–1676

Valente AP, Miyamoto CA, Almeida FCL (2006) Implications of protein conformational diversity for binding and development of new biological active compounds. Curr Med Chem 13:3697–3703

Wahl MC, Irmler A, Hecker B, Schirmer RH, Becker K (2005) Comparative structural analysis of oxidized and reduced thioredoxin from *Drosophila melanogaster*. J Mol Biol 345:1119–1130